Technical Physics, 2023, Vol. 68, No. 7

13

Features of the course of the solid-state reactions in a Sn/Fe/Cu trilayer film system

© Yu.Yu. Balashov,[1] V.G. Myagkov,[1] L.E. Bykova,[1] M.N. Volochaev,[1] V.S. Zhigalov,[1] A.A. Matsynin,[1] K.A. Galushka,[2] G.N. Bondarenko,[1] S.V. Komogortsev[1]

[1] Kirensky Institute of Physics, Federal Research Center KSC SB, Russian Academy of Sciences,
660036 Krasnoyarsk, Russia
[2] Siberian Federal University,
660041 Krasnoyarsk, Russia
e-mail: y.balashov@yandex.ru

Received April 6, 2023
Revised April 6, 2023
Accepted April 6, 2023

Study of the mechanisms of the solid-state reactions in Sn/Fe/Cu thin films is interesting both from a fundamental point of view and from a view of the importance of emerging intermetallics in the technology of solder joints and thin-film lithium-ion batteries. By the integrated approach, including both X-ray phase analysis and local elemental analysis of the cross-sections of the films, the phase composition and the mutual arrangement of phases were studied, at various stages of the solid-state reaction occurring at different temperatures. The observed sequence of the appearing phases differs significantly from the expected one if the mass transfer took place by a volume diffusion through the forming layers.

Keywords: thin films, transmission electron microscopy, energy dispersion spectroscopy, mass transfer mechanisms.

DOI: 10.61011/TP.2023.07.56642.73-23

Introduction

The problem of stability of operation of multilayer thin-film systems in nanoelectronics brings to the forefront the necessity of examination of diffusion and solid-state chemical reactions in thin films containing several layers differing in their chemical composition. The fundamental principles of solid-state chemical transformations are also being studied extensively. Bi- and trilayer films with atomic transport presumably being essentially one-dimensional are methodologically convenient objects for such research.

The examination of solid-state reactions in thin films has already revealed a number of new laws, such as the first-phase rule [1,2]; low (compared to bulk samples) reaction temperatures [3]; and a high atomic transfer rate.

The observation of unexpected mutual positioning of emerging phases [1,4] is one of the intriguing findings made in studies into metallic trilayer films. The peculiarity, which was examined in [1] for Ge/Ag/Mn films, consists in the fact that intermetallic compounds forming in bilayer films, which consist of just the top and bottom layers of a trilayer system, also form in a trilayer system, and the buffer layer turns out to be chemically pure.

Diffusion is typically regarded as a mechanism of atomic transfer in solid-state reactions. However, experimentally observed high transformation rates and other features [1,4] suggest that diffusion is not the only (and, in certain cases, the primary) transfer mechanism.

Data on solid-state reactions in thin Sn/Fe/Cu films are of interest not only in the context of accumulation of experimental knowledge in solid-state chemistry. The mechanisms of formation of intermetallic compounds in such systems (Cu_6Sn_5, $FeSn_2$, and FeSn) are relevant to the technology of both solder joints [5–7] and thin-film lithium-ion batteries [8–10].

In the present study, local elemental analysis of the cross section of a Sn(400 nm)/Fe(170 nm)/Cu(300 nm) trilayer film with a transmission electron microscope is used to examine the mutual positioning of phases at different stages of a solid-state reaction proceeding at different temperatures. This approach provides a unique opportunity to identify the mutual positioning of phases in products of solid-state reactions [7,11]. This study is a logical continuation of research into solid-state reactions in bilayer Sn/Fe [12] and Sn/Cu [13,14] film systems, which allowed us to determine the sequence and certain specific features of solid-state reactions in Sn–Fe and Sn–Cu layer pairs.

1. Experimental technique and sample preparation

Two different trilayer Sn/Fe/Cu films were used in the study: a Sn(130 nm)/Fe(70 nm)/Cu(160 nm) film on a sitall substrate („series A") and a Sn(400 nm)/Fe(170 nm)/Cu(300 nm) film on a single-crystal MgO substrate („series B"). Trilayer films were fabricated

by thermal deposition in vacuum under a residual pressure of $1.3 \cdot 10^{-4}$ Pa at room temperature. High-purity materials were used for sputtering: Cu (99.99%), Fe (99.99%), and Sn (99.995%). The thickness of Sn and Cu layers was monitored by X-ray fluorescence analysis. Samples were annealed also under $1.3 \cdot 10^{-4}$ Pa at different temperatures for 40 min (series A) or 30 min (series B). The phase composition was examined with a DRON-4.07 diffractometer and CuK_α radiation (the wavelength was 0.15418 nm). Energy-dispersive X-ray spectroscopy was used to perform local elemental analysis of cross sections of films. A Hitachi HT7700 transmission electron microscope fitted with a Bruker X-Flash 6T/60 energy-dispersive spectrometer was used in these studies. Cross sections were prepared by a Hitachi FB2100 single-beam FIB (focused ion beam) system. All measurements were performed at room temperature. The temperature dependence of electric resistance of films was measured using the four-point probe method with pressure contacts in vacuum ($1.3 \cdot 10^{-4}$ Pa) at a constant rate of heating and subsequent cooling ($\sim 4^\circ$C/min). The accuracy of both resistance and temperature measurements was ± 0.5%.

2. Experimental results and discussion

The variation of resistance of the Sn(160 nm)/Fe(70 nm)/Cu(130 nm) film with temperature (Fig. 1) is indicative of irreversible processes (solid-state reactions) at temperatures above 100°C. The characteristic temperatures of the onset of various transformations correspond to noticeable deviations from a linear reversible resistance growth. For example, the resistance decreases at 100°C; as will be shown below, this is related to the formation of a Cu_6Sn_5 phase. A resistance jump is seen around the melting temperature of tin ($\sim 230^\circ$C). The characteristic temperatures noted in resistance variations suggest the choice of temperatures for further analysis of the phase composition (a pitch of 100°C). A smaller annealing temperature increment (50°C) was used to analyze cross sections.

The results of examination of the phase composition (Fig. 2) yield the following phase sequence for series A:

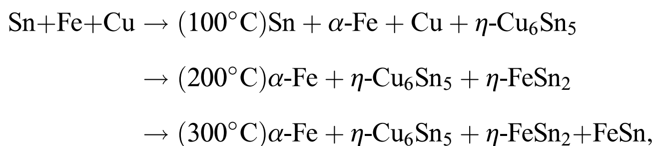

$$\mathrm{Sn+Fe+Cu} \rightarrow (100^\circ\mathrm{C})\mathrm{Sn} + \alpha\text{-Fe} + \mathrm{Cu} + \eta\text{-}\mathrm{Cu_6Sn_5} \rightarrow (200^\circ\mathrm{C})\alpha\text{-Fe} + \eta\text{-}\mathrm{Cu_6Sn_5} + \eta\text{-}\mathrm{FeSn_2} \rightarrow (300^\circ\mathrm{C})\alpha\text{-Fe} + \eta\text{-}\mathrm{Cu_6Sn_5} + \eta\text{-}\mathrm{FeSn_2}+\mathrm{FeSn},$$

while the sequence for series B is

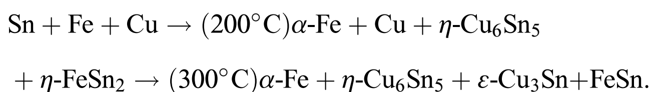

$$\mathrm{Sn + Fe + Cu} \rightarrow (200^\circ\mathrm{C})\alpha\text{-Fe} + \mathrm{Cu} + \eta\text{-}\mathrm{Cu_6Sn_5} + \eta\text{-}\mathrm{FeSn_2} \rightarrow (300^\circ\mathrm{C})\alpha\text{-Fe} + \eta\text{-}\mathrm{Cu_6Sn_5} + \varepsilon\text{-}\mathrm{Cu_3Sn}+\mathrm{FeSn}.$$

Diffraction reflections of phases were identified as β-Sn (PDF Card № 00-004-0673); Fe (PDF Card № 06-696) and Cu (PDF Card № 00-004-0836); η-Cu_6Sn_5 (PDF Card № 00-047-1575); $FeSn_2$ (PDF Card № 04-001-0929); FeSn (PDF Card № 01-076-8244).

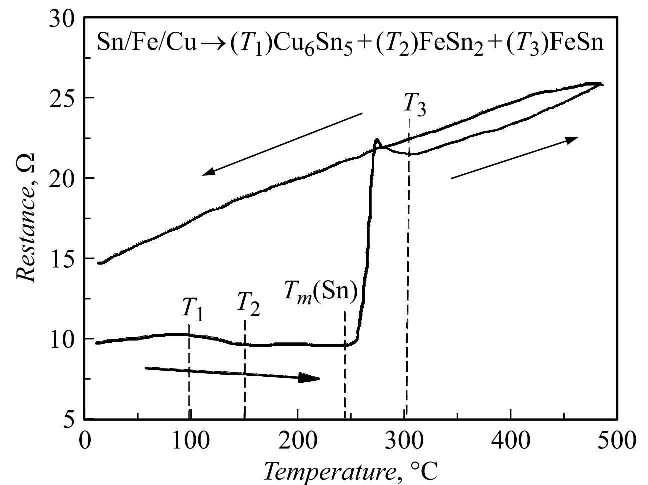

Figure 1. Variation of resistance of the Sn(160 nm)/Fe(70 nm)/Cu(130 nm) film with annealing temperature.

Note that even though Cu and Sn are separated by a Fe layer, annealing of the Sn(160 nm)/Fe(70 nm)/ Cu(130 nm) film at 100°C resulted in the formation of just the η-Cu_6Sn_5 phase. The temperature of initiation of a reaction producing the η-Cu_6Sn_5 phase determined in studies into the formation of η-Cu_6Sn_5 intermetallic films in bilayer Sn/Cu thin films [13,14] was also $T_{\text{in}} \sim 100^\circ$C. Initiation temperatures of $\sim 150^\circ$C for $FeSn_2$ and $\sim 300^\circ$C for FeSn in Sn/Fe films have been determined earlier [12]. Only the reflections from phases Cu_6Sn_5, $FeSn_2$, and FeSn are seen in the diffraction pattern after annealing at 400°C; the reflections from copper, iron, and tin vanish completely. Interestingly, the film structure obtained at the end of thermal processing of series A consists of $Cu_6Sn_5 + FeSn_2 +$ FeSn intermetallic compounds, which hold promise for the fabrication of anodes of thin-film solid-state lithium-ion batteries [8–10]. The phase sequences for series A and B differ due to the fact that the process of reaction between film reagents is governed not only by the nature of reagents themselves, but also by the layer thickness and the structure of a substrate. For example, a single-crystal substrate (MgO) facilitates the growth of a deposited film with a pronounced texture and a lower defect density [15]. An amorphous substrate implies a lack of texture and an increased density of defects in a film. Alongside with the variation of layer thicknesses, this affects the parameters of component mass transfer. In the present case, this is manifested in the difference between the reaction initiation temperatures for series A and B, which agrees with the results of studies into reactions in ternary thin-film systems with an inert buffer layer between reagents [1,4]. This also helps one understand why the temperature at which a copper layer reacts completely to form an intermetallic layer in series A is lower than in series B. When the temperature exceeds 200°C, Cu_3Sn forms in series B, but this intermetallic

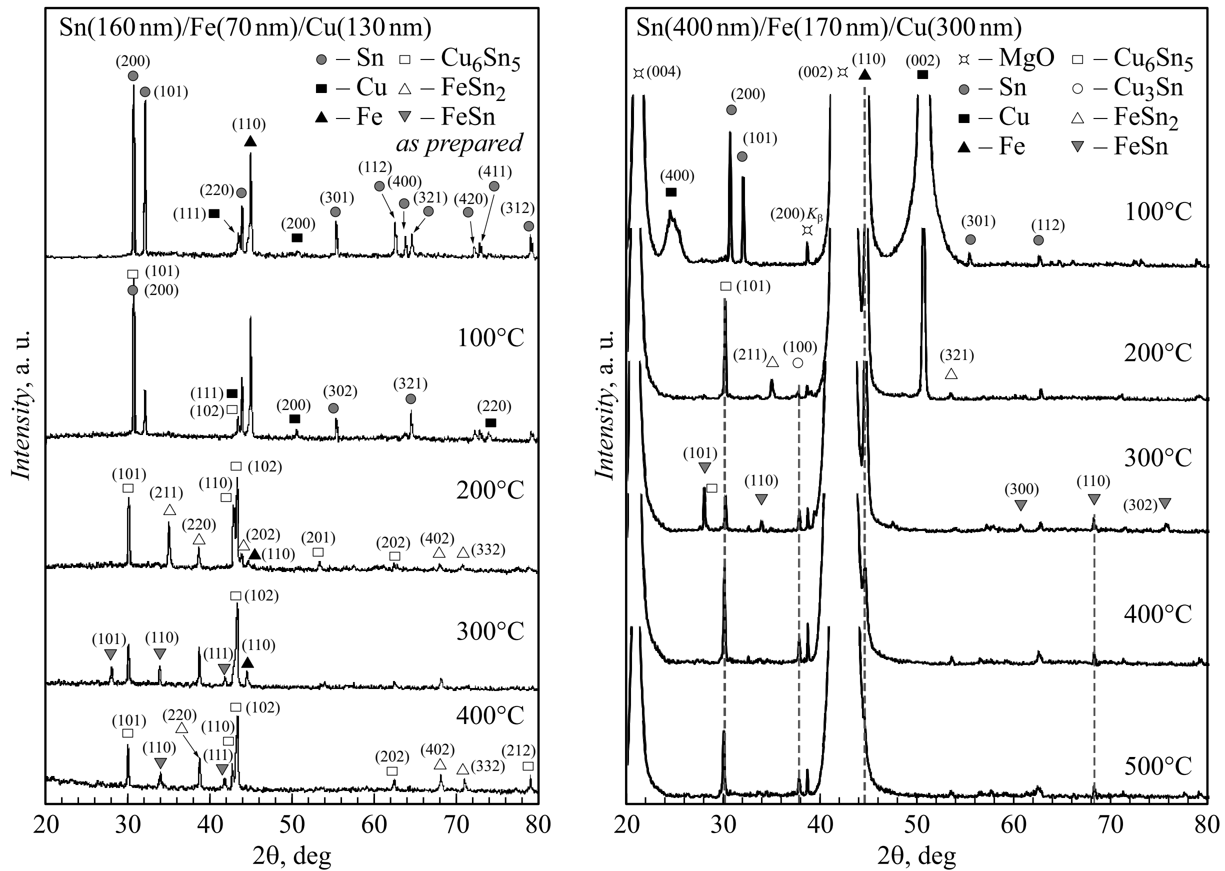

Figure 2. Diffraction patterns of the Sn(160 nm)/Fe(70 nm)/Cu(130 nm) film annealed from room temperature to 400°C and the Sn(400 nm)/Fe(170 nm)/Cu(300 nm) film annealed from room temperature to 500°C.

compound is not observed in series A at any annealing temperature, since copper reserves needed for its formation are already exhausted.

The boundaries of crystallites and layers are seen clearly in the images of film cross sections for series B (Fig. 3). The results of local elemental analysis along the film thickness reveal a uniform distribution of elements Sn, Fe, and Cu within each layer and a sharp change in their concentration at the interfaces between layers. Having compared the obtained atomic concentrations within each layer to the stoichiometric ratios in phases determined by X-ray diffraction (XRD) analysis, we found the following mutual positioning of layers of forming phases:

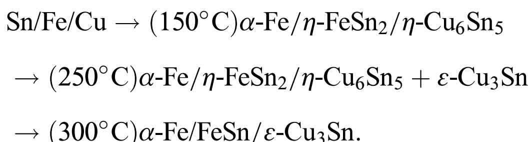

$$\text{Sn/Fe/Cu} \rightarrow (150^\circ\text{C})\alpha\text{-Fe}/\eta\text{-FeSn}_2/\eta\text{-Cu}_6\text{Sn}_5$$
$$\rightarrow (250^\circ\text{C})\alpha\text{-Fe}/\eta\text{-FeSn}_2/\eta\text{-Cu}_6\text{Sn}_5 + \varepsilon\text{-Cu}_3\text{Sn}$$
$$\rightarrow (300^\circ\text{C})\alpha\text{-Fe/FeSn}/\varepsilon\text{-Cu}_3\text{Sn}.$$

The mutual positioning of layers η-Cu_6Sn_5 and η-$FeSn_2$, which form in the process of annealing at 150°C, and layer α-Fe (Fig. 3) appears unusual. It seems natural that a Fe_mSn_n/Fe/Cu-type structure should form first in a solid-state reaction with atomic transfer effected by diffusion. However, it follows from experimental data for annealing at 150°C that a Fe layer in on top, while the bottom layer is η-Cu_6Sn_5. Note that a η-Cu_6Sn_5 layer could form only via transfer of tin atoms through a α-Fe layer, and the positioning of layers α-Fe and η-$FeSn_2$ (α-Fe/η-$FeSn_2$) turns out to be inverted relative to the initial order of Sn/Fe layers. This „peculiarity“ of the sequence of solid-state reactions and mutual positioning of phases has been observed earlier [1,4] and may be attributed both to uncommon mechanisms of atomic transport and to unordinary interatomic interactions [4]. It is also well-known that Cu is the primary diffusing component in a Cu-Sn binary system [16]. The mutual positioning of layers observed in the present case suggests that atomic transport is effected by Sn. It has been demonstrated in the study of kinetics of reactive diffusion in a solid−Fe/liquid−Sn system [17] that a $FeSn_2$ phase in the form of a layer with a columnar microstructure, which accelerates the migration of Sn and Fe atoms, forms in the process of annealing of Fe/Sn diffusion pairs within the 703−773 K temperature range. Note that it is reasonable to expect, e.g., capillary transfer through triple junctions of grains to be established alongside with diffusion transfer under such conditions in a system with a low-melting component.

A certain discrepancy between the phase composition observed in cross-section images and XRD data may be

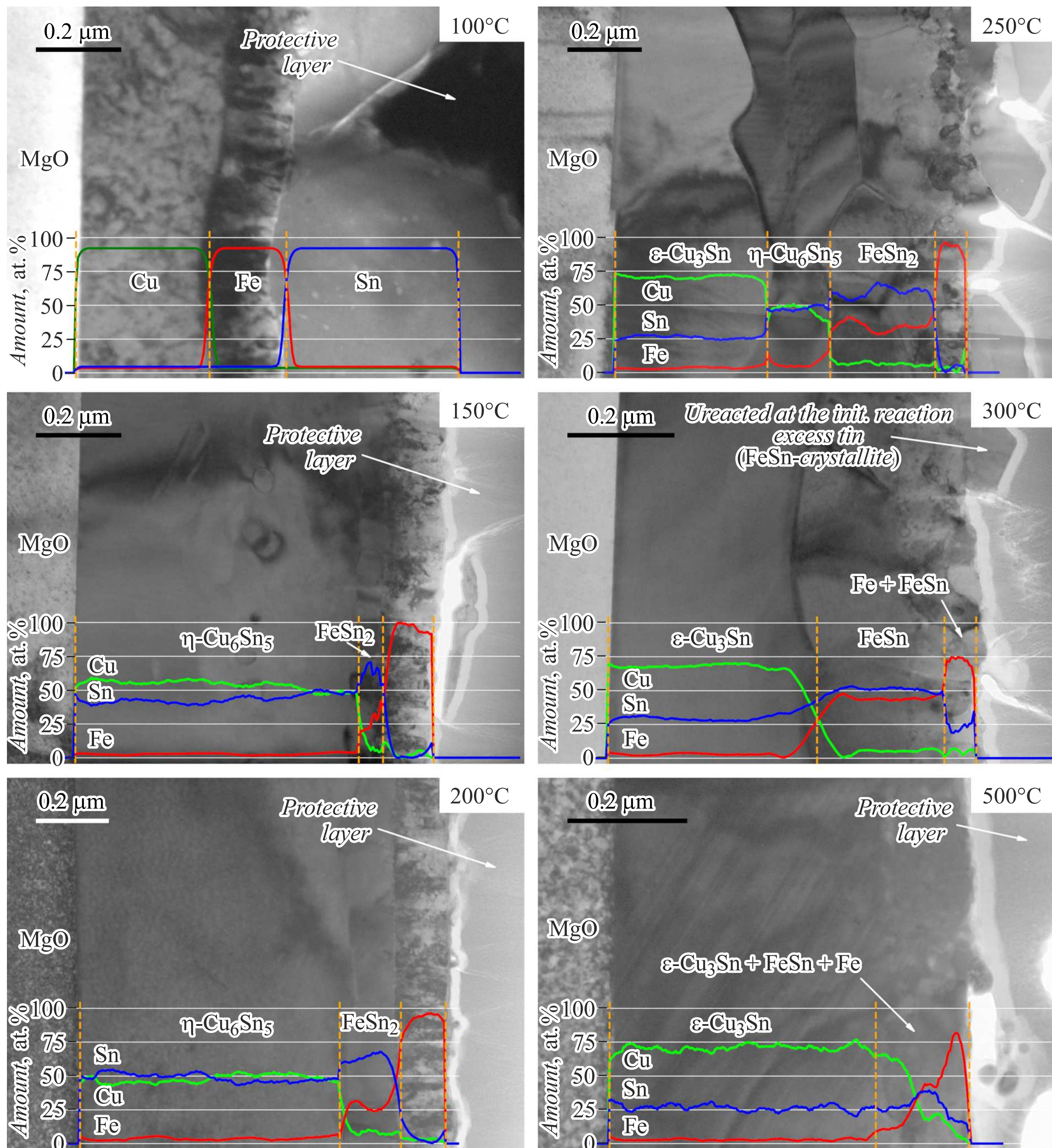

Figure 3. Cross sections of films after annealing at different temperatures (100−500°C) with superimposed plots of variation of the atomic ratio of elements Sn, Fe, and Cu along the thickness of samples.

attributed to the locality of measurements with an energy-dispersive spectrometer. The thickness nonuniformity of the Sn layer in the as-prepared film (Fig. 3, 100°C) is the reason behind nonuniformity of the phase composition over the area of the annealed film. Note that this thickness nonuniformity of the Sn layer did not hinder the formation of uniform-thickness layers in the course of annealing (Fig. 3, temperatures in excess of 100°C).

Macropores, which reduce the strength of electric contacts [7,18], often form at the Cu_3Sn/Cu_6Sn_5 phase interfaces emerging in a Sn−Cu system due to the Kirkendall effect. Interestingly, no such pores were observed in the present study. These pores should form in a reaction at interface η-Cu_6Sn_5/Cu $\rightarrow$ η-Cu_6Sn_5/ε-Cu_3Sn/Cu due to a considerable difference in density between the emerging ε-Cu_3Sn compound and phase η-Cu_6Sn_5. Apparently, introduced iron reduces the intensity of the flux of atoms to the reaction zone, shifting the process of phase growth closer to equilibrium (and reducing the number of defects). Consequently, pores, which emerge as dislocations flow

to grain boundaries that reduce the stress caused by the difference in density of adjacent phases, do not form. This fact may be used to enhance the strength of solder joints.

Conclusion

The phase composition and mutual positioning of phases at different stages of a solid-state reaction proceeding at various temperatures in Sn/Fe/Cu films were examined using a complex approach that involved X-ray diffraction analysis and local elemental analysis of cross sections of films. It was demonstrated that film structures with different layer thicknesses and substrates have different sequences of phases forming at gradually increasing annealing temperatures. The observed sequence of forming phases differs considerably from the expected one in the case when mass transfer is effected by volume diffusion through forming layers. In addition, it was found that phase Cu_6Sn_5 formed first and, although Cu is the primary diffusing component in a Cu/Sn binary system, the atomic transfer in the discussed experiments was effected by Sn.

Conflict of interest

The authors declare that they have no conflict of interest.

References

[1] V.G. Myagkov, L.E. Bykova, A.A. Matsynin, M.N. Volochaev, V.S. Zhigalov, I.A. Tambasov, Yu.L. Mikhlin, D.A. Velikanov, G.N. Bondarenko. J. Solid State Chem., **246**, 379 (2017). DOI: 10.1016/j.jssc.2016.12.010
[2] E.G. Colgan. Mater. Sci. Reports, **5**, 1 (1990). DOI: 10.1016/S0920-2307(05)80005-2
[3] D.P. Adams. Thin Solid Films, **576**, 98 (2015). DOI: 10.1016/j.tsf.2014.09.042
[4] V. Myagkov, O. Bayukov, Yu. Mikhlin, V. Zhigalov, L. Bykova, G. Bondarenko. Philos. Mag., **94**, 2595 (2014). DOI: 10.1080/14786435.2014.926037
[5] J. Görlich, G. Schmitz, K.N. Tu. Appl. Phys. Lett., **86**, 053106 (2005). DOI: 10.1063/1.1852724
[6] Y.Q. Wu, S.D. McDonald, J. Read, H. Huang, K. Nogita. Scripta Mater., **68**, 595 (2013). DOI: 10.1016/j.scriptamat.2012.12.012
[7] P.Y. Chia, A.S.M.A. Haseeb. J. Mater Sci: Mat. Electron., **26**, 294 (2015). DOI: 10.1007/s10854-014-2398-9
[8] W.H. Pu, X.M. He, J.G. Ren, C.R. Wan, C.Y. Jiang. Electrochim. Acta., **50**, 4140 (2005). DOI: 10.1016/j.electacta.2005.01.041
[9] O. Mao, R.A. Dunlap, J.R. Dahn. J. Electrochem. Soc., **146**, 405 (1999). DOI: 10.1149/1.1391622
[10] O. Mao, J.R. Dahn. J. Electrochem. Soc., **146**, 414 (1999). DOI: 10.1007/s10854-014-2398-9
[11] H. Shao, A. Wu, Y. Bao, Y. Zhao, G. Zou, L. Liu. Microelectron. Reliability, **91**, 38 (2018). DOI: 10.1016/j.microrel.2018.08.004
[12] V.G. Myagkov, V.S. Zhigalov, L.E. Bykova, L.A. Solovyov, A.A. Matsynin, Yu.Yu. Balashov, I.V. Nemtsev, A.V. Shabanov, G.N. Bondarenko. J. Mater. Res., **36**, 3121 (2021). DOI: 10.1557/s43578-021-00312-4
[13] L.E. Bykova, S.M. Zharkov, V.G. Myagkov, Yu.Yu. Balashov, G.S. Patrin. Phys. Solid State, **64** (2), 33 (2022). DOI: 10.21883/FTT.2021.12.51685.139
[14] L.E. Bykova, V.G. Myagkov, Y.Y. Balashov, V.S. Zhigalov, G.S. Patrin. J. Sib. Fed. Univ. Math. Phys., **15** (4), 493 (2022). DOI: 10.17516/1997-1397-2022-15-4-493-499
[15] J.M. Purswani, T. Spila, D. Gall. Thin Solid Films, **515**, 1166 (2006). DOI: 10.1016/j.tsf.2006.07.142
[16] K.N. Tu, R.D. Thompson. Acta Metall, **30**, 947 (1982). DOI: 10.1016/0001-6160(82)90201-2
[17] M. Hida, M. Kajihara. Mater. Trans., **53**, 1240 (2012). DOI: 10.2320/matertrans.M2012060
[18] V. Vuorinen, T. Laurila, T. Mattila, E. Heikinheimo, J.K. Kivilahti. J. Electron. Mater., **36**, 1355 (2007). DOI: 10.1007/s11664-007-0251-0

Translated by D.Safin